Published in final edited form as:
Leuk Lymphoma. 2010 April ; 51(4): 702–714. doi:10.3109/10428191003646697.

Osteolytic bone resorption in adult T-cell leukemia/lymphoma

Sherry T. Shu[1,2], **Chelsea K. Martin**[1], **Nanda K. Thudi**[1], **Wessel P. Dirksen**[1,2], and **Thomas J. Rosol**[1,2,3]

[1]Department of Veterinary Biosciences, The Ohio State University, Columbus, OH, USA

[2]Center for Retrovirus Research, The Ohio State University, Columbus, OH, USA

[3]Comprehensive Cancer Center, Arthur G. James Cancer Hospital and Solove Research Institute, The Ohio State University, Columbus, OH, USA

Abstract

Adult T-cell leukemia/lymphoma (ATLL) is caused by human T lymphotropic virus type 1 (HTLV-1). Patients with ATLL frequently develop humoral hypercalcemia of malignancy (HHM) resulting from increased osteoclastic bone resorption. Our goal was to investigate the mechanisms of ATLL-induced osteoclastic bone resorption. Murine calvaria co-cultured with HTLV-1-infected cells directly or conditioned media from cell cultures had increased osteoclast activity that was dependent on RANKL, indicating that factors secreted from ATLL cells had a stimulatory effect on bone resorption. Factors released from resorbing bone stimulated proliferation of HTLV-1-infected T-cells. Parathyroid hormone-related protein (PTHrP) and macrophage inflammatory protein-1α (MIP-1α), both osteoclast stimulators, were expressed in HTLV-1-infected T-cell lines. Interestingly, when HTLV-1-infected T-cells were co-cultured with pre-osteoblasts, the expression of osteoprotegerin (OPG), an osteoclast inhibitory factor, was significantly down-regulated in the pre-osteoblasts. When OPG was added into the *ex vivo* osteoclastogenesis assay induced by HTLV-1-infected T-cells, osteoclastogenesis was strongly inhibited. In addition, HTLV-1-infected T-cells inhibited expression of early osteoblast genes and induced late genes. These regulators will serve as future therapeutic targets for the treatments of HHM in ATLL.

Keywords

Osteolytic bone resorption; PTHrP; MIP-1α; RANKL; OPG; ATLL

Introduction

Humoral hypercalcemia of malignancy (HHM) is a common metabolic complication of solid cancers [1]. Most hematological malignancies are uncommonly associated with HHM; however, approximately 80% of patients with adult T-cell leukemia/lymphoma (ATLL) develop hypercalcemia associated with severe osteolytic lesions [2]. ATLL is a fatal malignancy caused by human T lymphotropic virus type 1 (HTLV-1). The high incidence of HHM in patients with ATLL contributes to a very poor median survival, which is about 6 months. However, the mechanisms of HHM in ATLL and the bone–ATLL cell interactions are not well understood.

Correspondence: Thomas J. Rosol, 1925 Coffey Road, Columbus, OH 43214, USA. Tel: 614-292-4265. Fax: 614-292-6473. rosol.1@osu.edu.

The bone–cancer cell interaction has been described as a 'vicious cycle' where cancer cells increase the activity of osteoclasts to induce bone resorption, and the release of growth factors from osteolytic bone supports further tumor progression [3]. Tumor-derived bone stimulating factors include osteolytic factors such as parathyroid hormone-related protein (PTHrP), transforming growth factor-β (TGF-β), and interleukin-11 (IL-11), among others [4]. Cancer cells also express osteoblastic factors including vascular endothelial growth factor (VEGF), platelet-derived growth factor (PDGF), and endothelin-1 (ET-1) [4]. Factors released from bone undergoing resorption (bone-derived growth factors) include TGF-β and insulin-like growth factors (IGFs), which are known to facilitate the growth and metastasis of cancer cells [4]. Furthermore, the process of bone remodeling (local sequential bone resorption and formation) results in a microenvironment ideal for cancer-cell growth, metastasis, and development of drug resistance. Features of the remodeling-bone microenvironment include hypoxia, acidosis, and increased extracellular calcium concentration resulting in calcium-sensing receptor signaling [4].

The 'vicious cycle' phenomenon has been extensively studied in breast cancer, prostate cancer, multiple myeloma, B cell lymphoma [5], and other tumors that metastasize to bone. Most patients with ATLL (80%) develop HHM, and osteolytic lesions frequently occur in these patients. High levels of PTHrP, macrophage inflammatory protein-1α (MIP-1α), IL-1, IL-6, and tumor necrosis factor-α (TNF-α) are typically present in the serum from patients with ATLL and HHM. Transgenic mice that express the HTLV-1 viral oncoprotein, Tax, form tumors which express receptor activator of nuclear factor-κB ligand (RANKL), TGF-β, PDGF, and IL-6 [6]. These factors have all been shown to be important in bone remodeling; nevertheless, the 'vicious cycle' in ATLL, which is likely to be humorally regulated, is not well characterized. Here we demonstrate the significance of the tumor-derived bone-stimulating factors and bone-derived growth factors in bone–ATLL cell interaction using an *ex vivo* model of bone resorption. The results from this study will increase our understanding of the pathogenesis of osteolysis and HHM in ATLL, which should lead to improved future therapies.

Materials and methods

Cells and reagents

RV-ATL, ED, TL and Hut102 are cell lines derived from ATLL patients [7]. RV-ATL cells were super-infected by HTLV-1 to develop the HT1RV cell line. HTLV-1-infected cell lines (MT-2, SLB-1, and C8166), HTLV-1-negative T-cells (Jurkat), Hut102, and HT1RV cells were cultured as previously described [8]. The murine pre-osteoclast cell line RAW 264.7 was a generous gift from Dr. Michael Ostrowski at The Ohio State University, and cells were cultured in RPMI medium containing 5% fetal bovine serum (FBS), 50 μg/mL penicillin/streptomycin, and 4 mM L-glutamine [9]. Murine pre-osteoblast cell lines, MC3T3 and ST2, were cultured in α-minimum essential medium (αMEM) containing 10% FBS, 50 μg/mL penicillin/streptomycin, and 4 mM L-glutamine.

Cell viability assays

Cell viability was measured using a CellTiter 96® non-radioactive cell proliferation assay kit (Promega, WI) according to the manufacturer's protocol.

RNA extraction, reverse transcription, PCR, and real-time PCR

RNA extraction, reverse transcription (RT), polymerase chain reaction (PCR), and real-time PCR were performed as previously described [10–12]. The murine primers for real-time RT-PCR included β_2-microglobulin (B2M) (forward: AGA GTT AAG CAT GCC AGT ATG G and reverse: ACT GGA TTT GTA ATT AAG CAG GTT C), matrix metalloproteinase-9

(MMP-9) (forward: CAT TCG CGT GGA TAA GGA GT and reverse: ATT TTG GAA ACT CAC ACG CC), MMP-10 (forward: TTT TCC AGG AAT TGA GCC AC and reverse: CAT TGG GGT CAA ACT CGA AC), osteopontin (forward: GCT TGG CTT ATG GAC TGA GG and reverse: CGC TCT TCA TGT GAG AGG TG), osteocalcin (forward: CTC ACA GAT GCC AAG CCC and reverse: CCA AGG TAG CGC CGG AGT CT), PTHrP (forward: AGT GTC CTG GTA TTC CTG CTC and reverse: ATG CAG TAG CTG ATG TTC AGA CAC), runt-related transcription factor-2 (RUNX2) (forward: CGA CAG TCC CAA CTT CCT GT and reverse: TAC CTC TCC GAG GGC TAC AA), macrophage colony-stimulating factor (M-CSF) (forward: ATG GAC ACC TGA AGG TCC TG and reverse: CAT CCA GCT GTT CCT GGT CT), RANKL (forward: ACA CCT CAC CAT CAA TGC T and reverse: CTT AAC GTC ATG TTA GAG ATC TTG G), osteoprotegerin (OPG) (forward: AGC TGC TGA AGC TGT GGA A and reverse: TCG AGT GGC CGA GAT), cathepsin K-1 (forward: CTT CCA ATA CGT GCA GCA GA and reverse: CCT CTG CAT TTA GCT GCC TT), macrophage colony-stimulating factor receptor (M-CSFR) (forward: CTC TCA GTA CTT CAG GGC CG and reverse: CAG CAG TAG CAC CAG CAG AG), and nuclear factor of activated T-cells (NFATc1) (forward: GGG ACA CAG CCC TAT CTT CA and reverse: AGG CTG TAC CTC GAT CCT CA).

Measurement of PTHrP and MIP-1α concentrations

Human MIP-1α concentrations were measured using a Human CCL3/MIP-1α Quantikine ELISA (enzyme-linked immunosorbent assay) kit (R&D systems, MN). PTHrP concentrations were measured using an immunoradiometric assay (IRMA) kit (Diagnostic Systems Laboratories, Webster, TX).

Calvarial bone culture

Calvaria were harvested from 4–6-day-old mouse pups. Two calvarial bone disks were collected from each mouse using a 3.5 mm diameter biopsy punch. Calvarial disks were washed three times in basal medium consisting of BGJ_b culture medium (Invitrogen, CA) supplemented with 0.1% bovine serum albumin (BSA) (Sigma-Aldrich Corp., MO), 2 mM L-glutamine (Invitrogen), and 100 μg/mL Normocin (InvivoGen, San Diego, CA). Calvarial disks were cultured overnight in an incubator at 37°C and 5% CO_2 and supplemented with either 10 μM zoledronic acid (Novartis, Princeton, NJ) or vehicle. The following morning, calvarial disks were washed, and six disks were randomly assigned to each treatment group and cultured for 6 days. Cultures of calvarial disks with either 10 nM parathyroid hormone (PTH) (Calbiochem, CA) or 2 ng/mL IL-1α served as positive controls. Conditioned medium was harvested from 48 h HTLV-1-infected and -non-infected lymphocyte cultures (in RPMI medium; Invitrogen, CA) and co-cultured with calvarial disks at a concentration of 25% conditioned medium in basal medium. Alternatively, calvarial bone was co-cultured in direct contact with HTLV-1-infected and -non-infected lymphocytes. On the sixth day of co-culture, medium was harvested and total calcium concentrations were determined using a Quanti-ChromTM Calcium Assay kit (BioAssay Systems, CA). Calvarial bone disks were fixed and stained for tartrate-resistant acid phosphatase (TRAP) activity using an acid phosphatase leukocyte kit (Sigma-Aldrich Corp., St. Louis, MO). Following TRAP staining, the calvarial bone disks were whole-mounted on glass slides using aqueous mounting medium and photographed. Alternatively, calvarial disks were imaged by microcomputed tomography (μCT, Inveon; Siemens) and total bone volume was measured. μCT scanning was supported by the Wright Center of Innovation in Biomedical Imaging at The Ohio State University.

Pre-osteoclasts and pre-osteoblasts co-cultured with T-cells

RAW 264.7 cells (200 000 cells), ST2 cells (10 000 cells), or MC3T3 cells (10 000 cells) were plated in six-well plates (Corning, Lowell, MA) and allowed to attach overnight.

HTLV-1-positive T-cells (MT-2, SLB-1, C8166, Hut102, HT1RV, ED, and TL cells, 200 000 cells) or HTLV-1-negative T-cells (Jurkat, 200 000 cells) were cultured in cell culture inserts with 0.4 μm pore size (Millipore, MA) and co-cultured with RAW 264.7, ST2, or MC3T3 cells for 3 days. Conditioned medium was collected and assayed with a murine OPG ELISA (R&D Systems, Minneapolis, MN). RNA was isolated from the co-cultured RAW 264.7, ST2, and MC3T3 cells for real-time RT-PCR and mouse osteogenesis PCR array assays (SABiosciences, Frederick, MD).

Murine OPG ELISA assay

OPG concentrations in the conditioned media were measured using a murine OPG ELISA kit from R&D Systems according to the manufacturer's protocol.

Mouse osteogenesis PCR array

RNA from ST2 cells co-cultured with C8166 cells was treated with DNase using the Turbo DNA-*free*™ kit (Applied Biosystems, CA) and reverse transcribed using a RT^2 First Strand Kit (SA-Bioscience). The cDNA was mixed with RT^2 SYBR Green qPCR Mater Mix (SABioscience) and assayed using a Mouse Osteogenesis RT^2 Profiler™ PCR Array (SABioscience). Data analysis was performed using PCR Array Data Analysis Software (SABioscience).

In vitro osteoclastogenesis

Femoral bone marrow from 6–8-week-old mice was extracted, and 4×10^5 bone marrow mononuclear cells (BMMCs) were co-cultured with 1×10^4 Jurkat cells or C8166 cells using cell culture inserts with 0.4 μm pore size (Millipore, Billerica, MA) in αMEM and RPMI media (50% each; Invitrogen) containing 10% fetal calf serum (FCS) and 50 ng/mL of M-CSF for 12 days. Culture plates were fixed and stained for TRAP (Sigma-Aldrich Corp). The number of TRAP-positive multinucleated cells (osteoclasts) was counted by light microscopy [13].

Statistical analysis

Student's *t*-tests and analyses of variance (ANOVAs) were used for the statistical analysis. Pairwise comparisons were tested by Tukey's and Dunnett's methods to adjust for multiplicity. The symbol '*' indicates $p < 0.05$ and error bars indicate standard deviations, unless otherwise noted.

Results

Medium calcium concentration as a measure of osteoclast activity *ex vivo*

To model *in vivo* osteoclast activity in the bone microenvironment, 3.5 mm diameter disks of neonatal murine calvaria were cultured *ex vivo* in the presence of the osteoclast activators, PTH or IL-1. As a negative control, calvarial bone was treated overnight with zoledronic acid, a potent bisphosphonate and osteoclast inhibitor. Calcium concentrations in the culture medium were measured as an indicator of osteoclastic bone resorption. As expected, we found that the concentration of calcium in culture medium was significantly increased when calvarial bone was treated with PTH or IL-1, and significantly decreased when calvarial bone was treated with zoledronic acid [Figure 1(A)]. The zoledronic acid-mediated inhibition of osteoclastic bone resorption was not reversed by the addition of PTH or IL-1 [Figure 1(A)]. Increased medium calcium concentrations were due to increased osteoclast activity (measured by histochemical staining of TRAP-positive osteoclasts in whole-mounted calvarial bones) and loss of calvarial bone area [Figure 1(B)]. It was found that

medium calcium concentrations were a reliable indicator of osteoclast activity in *ex vivo* cultures of neonatal mouse calvarial bones.

HTLV-1-infected cells induced osteoclast activity *ex vivo*

To examine the effects of HTLV-1-infected cells on bone resorption, neonatal murine calvaria were co-cultured with conditioned media from HTLV-1-infected cells, or co-cultured in direct contact with HTLV-1-infected cells. Based on the calcium concentrations, calvarial bones cultured with conditioned media from HTLV-1-infected cells (MT-2, SLB-1, and C8166), or co-cultured directly with HTLV-1-infected cells (SLB-1 and C8166), had greater osteoclast activity when compared to calvarial bones cultured with unconditioned basal medium [Figures 2(A) and 2(B)]. This showed that factors secreted from HTLV-1-infected cells had a direct or indirect stimulatory effect on osteoclasts. There was no increase in calcium in the medium of HTLV-1-infected cells in the absence of calvarial bone [Figure 2(B)], indicating that the increase in calcium in the calvaria–cancer cell co-cultures was the result of increased osteoclast activity in the calvaria. The microstructure of bone resorption induced by HTLV-1-infected T-cells was examined by μCT, as shown in Figure 2(C). Total bone volume was measured, and a trend toward decreased total bone volume was found in calvaria co-cultured with HTLV-1-infected T-cells (SLB-1 and C8166).

Factors released from bone resulted in increased proliferation of HTLV-1-infected cells

To investigate whether factors released from bone affected the growth of HTLV-1-infected cells, conditioned medium from calvarial cultures was collected and added to HTLV-1-infected (MT-2 and SLB-1) and -negative (Jurkat) T-cell cultures. As shown in Figure 3, all three concentrations of calvaria-conditioned medium (25%, 50%, and 75%) increased the proliferation of HTLV-1-infected MT-2 and SLB-1 cells. In HTLV-1-negative Jurkat cells, only the 25% calvaria-conditioned medium mildly increased cellular proliferation. Increased proliferation of HTLV-1-infected cells in the presence of calvaria-conditioned medium indicated that bone factors may play an important role in supporting cancer cell proliferation in ATLL.

T-cells modulated gene expression in pre-osteoblasts

To examine the effects of T-cells on gene expression in osteoblasts and osteoclasts, HTLV-1-infected T-cells and HTLV-1-negative T-cells were co-cultured with the pre-osteoblast cell lines, ST2 and MC3T3. The characteristics of the HTLV-1-infected T-cell lines are listed in Table I. T-cells and pre-osteoblasts were separated by cell culture inserts to avoid direct contact during co-culture. RNA from the co-cultured ST2 and MC3T3 cells was isolated for real-time PCR analysis. As shown in Figure 4(A), the RANKL expression in ST2 cells co-cultured with SLB-1 and C8166 cells was significantly increased when compared to ST2 cells alone and ST2 cells co-cultured with HTLV-1-negative Jurkat T-cells. MC3T3 cells did not express detectable levels of RANKL with or without T-cell co-culture (data not shown). Importantly, OPG expression was significantly decreased in both ST2 and MC3T3 cells co-cultured with T-cells [Figures 4(B) and 4(C)]. OPG was decreased 5.4- and 12.8-fold in ST2 cells co-cultured with SLB-1 and C8166 cells, respectively, when compared to ST2 cells alone [Figure 4(B)]. The secreted levels of OPG were also low in the media from ST2 or MC3T3 cells co-cultured with Jurkat, SLB-1, and C8166 cells, compared to ST2 cells alone [(Figures 4(D) and 4(E)].

The expression levels of M-CSF, which is important for osteoclast development, were significantly decreased in ST2 cells co-cultured with SLB-1, C8166, TL, and ED cells when compared to ST2 cells alone [Figure 5(A)]. There were no significant changes in M-CSF expression in MC3T3 cells co-cultured with T-cells (data not shown). This suggests that M-CSF production by osteoblasts does not play a role in the increased bone resorption.

Interestingly, PTHrP expression was decreased in ST2 cells co-cultured with all the T-cell lines and MC3T3 cells co-cultured with MT-2, TL, and C8166 cells when compared to ST2 and MC3T3 cells alone [Figures 5(B) and 5(C)]. The expression of RUNX2, an important transcription factor that regulates osteoblast gene expression including OPG and RANKL, was decreased in ST2 cells co-cultured with MT-2, SLB-1, C8166, TL, and ED cells when compared to ST2 cells alone [Figure 5(D)]. No significant difference was found in RUNX2 expression in MC3T3 cells co-cultured with T-cells (data not shown). The expression of osteopontin, a glycoprotein important for anchoring osteoclasts to the mineral matrix of bone [15], was increased in ST2 cells co-cultured with Jurkat, SLB-1, C8166, and ED cells when compared to ST2 cells alone [Figure 5(E)]. The expression of osteocalcin, a non-collagenous biomarker of bone formation, was increased in ST2 cells co-cultured with Jurkat, SLB-1, and ED cells when compared to ST2 cells alone [Figure 5(F)]. These results indicate that the HTLV-1-infected cells inhibited the osteoblast early genes, PTHrP and RUNX2, but stimulated the osteoblast late genes, osteopontin and osteocalcin.

To investigate how T-cells affect global gene expression related to osteogenesis in pre-osteoblasts, a Mouse Osteogenesis RT^2 Profiler™ PCR Array was used. When comparing the gene expression in ST2 cells co-cultured with C8166 cells to ST2 cells alone, the expression of MMP-9 and MMP-10 was increased 5.2- and 6.9-fold, respectively. The results from the PCR array were confirmed by real-time RT-PCR [Figures 5(G) and 5(H)].

To investigate the effects of T-cells on gene expression in pre-osteoclasts, RAW 264.7 cells were co-cultured with T-cell lines (Table I). RNA from RAW 264.7 cells was isolated and real-time RT-PCR was performed. No significant differences in RANK, cathepsin K-1, M-CSFR, and NFATc1 gene expression were found when RAW 264.7 cells were co-cultured with T-cells (data not shown).

ATLL induced osteoclastic bone resorption through a RANKL-dependent pathway

To investigate whether the increased RANKL/OPG ratio in pre-osteoblasts co-cultured with HTLV-1-infected T-cells is the key mechanism of ATLL-induced osteoclastic bone resorption, the *ex vivo* osteoclastogenesis assay was performed using mouse BMMCs co-cultured with or without T-cells. The inhibitors for RANKL, recombinant OPG and RANKFc, were added into the culture and osteoclast-like cells identified by TRAP staining were counted. As shown in Figure 6, osteoclastogenesis was increased when BMMCs were co-cultured with HTLV-1-infected C8166 cells. When OPG or RANKFc was added into the cultures, osteoclastogenesis was strongly inhibited. These data indicated that the increased RANKL/OPG ratio in pre-osteoblasts is the key mechanism by which HTLV-1 induces osteoclastic bone resorption.

HTLV-1-infected T-cells expressed and secreted PTHrP and MIP-1α

To investigate the factors expressed and secreted from HTLV-1-infected T-cells that affect the bone microenvironment, real-time RT-PCR was performed to measure the mRNA expression of osteoclast activators (PTHrP, RANKL, and MIP-1α) and an osteoclast inhibitor (OPG). As shown in Figure 7 and Table I, PTHrP was expressed in the majority of the HTLV-1-infected T-cell lines examined. The expression level was highest in MT-2 cells (Figure 7). PTHrP secretion was also detected in the conditioned media from the cell cultures (Table I), but the concentrations of PTHrP did not always correlate with PTHrP mRNA. PTHrP can function as both an intracrine hormone (without secretion) and a secreted hormone. MIP-1α expression was detectable in the majority of the HTLV-1-infected T-cell lines, but the levels were very low in ED cells and HTLV-1-negative Jurkat T-cells (Figure 7). MIP-1α expression was high in MT-2, Hut102, SLB-1, and HT1RV cells (Figure 7). In addition, MIP-1α was secreted at high levels from Hut102, C8166, SLB-1,

MT-2, and HT1RV cells, at moderate levels from TL cells, and was undetectable in Jurkat cells (Table I). It has been reported that HTLV-1-infected T-cells expressed RANKL [16]; therefore, we measured the mRNA expression levels of RANKL and its decoy receptor OPG in T-cells (Figure 7). Detectable, but very low levels of RANKL were found in Hut102, SLB-1, and C8166 cells. The majority of the cell lines examined, except for ED cells, expressed detectable, but low levels of OPG. C8166 and HT1RV cells expressed higher levels of OPG compared to the other T-cell lines. These data indicated that the increased bone resorption in patients with ATLL likely results from multiple factors expressed from HTLV-1-infected T-cells.

Discussion

The ‘vicious cycle’ of cancer progression and bone resorption in ATLL is not yet completely understood. Here we demonstrated not only that factors secreted from HTLV-1-infected cells induce bone resorption, but also that bone releases factors that increase the proliferation of HTLV-1-infected T-cells. The majority of HTLV-1-infected T-cells expressed PTHrP and MIP-1α, indicating the importance of these two factors in the pathogenesis of HHM in patients with ATLL. PTHrP expression is increased in multiple cancers including breast cancer [17], prostate cancer [18], anaplastic thyroid cancer [19], ATLL [20], and many others [21]. The expression of PTHrP is regulated by various transcription factors at three promoter regions (P1, P2, and P3) [22]. In HTLV-1-infected cells, it has been reported that ETS-1, SP-1, and the P300/CBP complex can be recruited by the viral oncoprotein, Tax, to the P3 promoter of PTHrP and transactivate its transcription [8]. Constitutive activation of the NF-κB pathway in ATLL cells contributed to the transactivation of the PTHrP P2 promoter [23]. In addition to ETS-1 and NF-κB, PTHrP expression in breast cancer cells was up-regulated by TGF-β [22]. Interestingly, ATLL cells are known to express TGF-β [24]; however, the role of ATLL-derived TGF-β in PTHrP expression remains to be examined. We have demonstrated here that several HTLV-1-infected cell lines express PTHrP, while HTLV-1-negative cells did not [Table 1 and Figure 7]. The variation in the levels of PTHrP expression has been linked to the differential expression of Tax [8]; however, we did not find a correlation between Tax and PTHrP expression in this study (data not shown).

MIP-1α is a CC chemokine that attracts inflammatory cells and enhances their attachment to vascular endothelial cells. Increased levels of MIP-1α have been reported in cancer patients with multiple myeloma [8], Waldenström macroglobulinemia [25], Schwann cell tumors [26], and ATLL [13]. These tumors have the potential to develop bone metastases or bone lesions. The role of MIP-1α in multiple myeloma has been extensively studied. MIP-1α facilitates the survival of myeloma cells, increases the adhesion of myeloma cells to bone, induces osteoclastogenesis *in vitro*, and stimulates osteolytic lesions *in vivo* [10,27–29]. There are two receptors known to be important for MIP-1α function, namely, CCR1 and CCR5. Expression of CCR1, but not CCR5, was detected in several HTLV-1-infected cells (data not shown), and the expression of both CCR1 and CCR5 was found in human peripheral blood mononuclear cells (PBMCs) and bone marrow stromal cells [10], suggesting that the bone microenvironment can be affected by MIP-1α both directly and indirectly. The increase of osteoclast activity by MIP-1α has been linked to both RANKL-independent and -dependent pathways [10,29]; however, the mechanisms require further investigation.

We found that the majority of the HTLV-1-infected T-cell lines expressed and secreted PTHrP and MIP-1α (Table I and Figure 7). The secretion levels of PTHrP did not correlate well with its mRNA expression levels in the cells. It is known that the PTHrP gene contains a nuclear localization sequence (NLS), which induces translocation of the PTHrP protein

into the nucleus [30]. The gene expression profiles of PTHrP, MIP-1α, RANKL, and OPG and the data from calvaria *ex vivo* cultures indicate that the stimulatory effects of ATLL cells on bone resorption may result from the net effect of multiple factors, since both SLB-1 and C8166, the two cell lines that significantly induced *ex vivo* osteoclastic bone resorption, expressed all four genes.

PTHrP and TGF-β have been shown to play central roles in the vicious cycle induced by solid tumors, such as breast cancer. In lymphoma/leukemia, however, synergistic effects between various cytokines and PTHrP have been suggested. MIP-1α can enhance osteoclast formation induced by IL-6, PTHrP, and RANKL [10]. MIP-1α concentrations in serum have been shown to be an important biomarker for HHM in ATLL [13]. These results demonstrate that PTHrP and MIP-1α have significant roles in the 'vicious cycle' of cancer progression and osteolysis in patients with ATLL. However, we treated calvaria with exogenous MIP-1α or anti-MIP-1α antibodies without the stimulation of conditioned medium from HTLV-1-infected T-cell cultures, and found no change in osteoclast activity (data not shown), indicating that the induction of osteoclast activity by MIP-1α in cancers, such as multiple myeloma, may be the result of a synergistic relationship between MIP-1α and other factors such as PTHrP and RANKL [10].

It has been reported that RANKL expressed on ATLL cells plays an important role in HHM development [16]. Therefore, the very low expression of RANKL in HTLV-1-infected cell lines was unexpected. We observed only a slight increase in RANKL expression from pre-osteoblasts co-cultured with HTLV-1-infected SLB-1 and C8166 cells. However, the large decrease in OPG expression observed in co-cultured pre-osteoblasts may be more relevant. OPG expression can be affected by several factors. It has been shown that PTHrP increases RANKL but decreases OPG gene expression [31,32]. A single injection or infusion of PTH decreased OPG expression through the activation of cyclic adenosine monophosphate (cAMP) signal transduction [33]. TGF-β increased OPG gene expression in an osteoblastic cell line [34]. 1α,25-dihydroxyvitamin D3 suppressed OPG by accelerating the degradation of its mRNA and suppressing promoter activity through the AP-1 binding site by decreasing p-c-Jun in a JNK-independent pathway [34]. It has also been shown that T-cells decreased OPG expression of stromal cells through the binding of CD40L/CD40 [35]. In our co-culture system, T-cells and pre-osteoblasts were separated by cell culture inserts, suggesting that the down-regulation of OPG expression was induced by one or more secreted factors. In the future, it will be important to determine the identity of these secreted factors, and to elucidate how they down-regulate transcriptional activity of the OPG promoter.

MMPs are endopeptidases that participate in: (1) degradation of extracellular matrix (ECM) to permit cell migration; (2) alteration of the ECM microenvironment and cellular behavior; (3) modulation of biologically active molecules by direct cleavage or release from ECM stores; (4) regulation of the activity of other proteases; and (5) cell attachment, proliferation, differentiation, and apoptosis [36]. In bone, MMP-9 is essential for the migration of osteoclasts and their precursors during osteoclastogenesis. In cancer, an important role of MMPs is to degrade the ECM and stimulate the release of growth factors to allow the process of angiogenesis, tumor growth, and metastasis [37]. The role of MMPs in HTLV-1 infection has been discussed [38]. MMP-9 was detected in the cerebrospinal fluid (CSF) of patients with HTLV-1-induced tropical spastic paraparesis [39]. Astrocytes stimulated by HTLV-1-activated CD4+ T-cells secrete increased MMP-3 and MMP-9 through integrin-dependent and -independent pathways [40]. HTLV-1-infected T-cells secreted high levels of MMP-9, which is up-regulated by Tax through the NF-κB and SP2-1 signaling pathways [41]. MMP-9 may be responsible for the invasiveness of ATLL cells, since patients with disseminated organ involvement have higher MMP-9 levels when compared to patients with limited disease [41]. MMP-10 expression has been linked to the invasiveness of lung cancer

[42], renal cell carcinoma [43], esophageal squamous cell carcinoma [44], and prostate cancer [44]. Both MMP-9 and MMP-10 expression was found to be expressed by osteoblasts in bone [45]. Here we found that the expression of MMP-9, a gelatinase, and MMP-10, a stromelysin, were increased when ST2 cells were co-cultured with C8166 cells, suggesting that HTLV-1-infected T-cells not only express MMPs but also up-regulate the expression of MMPs in osteoblasts.

In conclusion, we demonstrated the importance of bone–ATLL cell interactions using an *ex vivo* neonatal murine calvarial bone culture system. ATLL cells secreted agonists of osteoclastic bone resorption, and resorbing bone released bone-derived growth factors, which further increased tumor cell proliferation. The increased RANKL/OPG expression in osteoblasts was essential for HTLV-1-induced osteoclastic bone resorption. In addition to PTHrP and MIP-1α, the pronounced reduction in OPG expression and the increased expression of MMPs and osteopontin during co-culture of pre-osteoblasts with HTLV-1-infected cells may represent potential targets for future therapeutic strategies.

Acknowledgments

The authors would like to thank Dr. Laurie McCauley at the University of Michigan for her critical review and Dr. Masao Matsuoka at Kyoto University and Dr. Owen O'Connor at Columbia University for providing ED and TL cell lines, respectively.

Declaration of interest: This work was supported by the National Cancer Institute (CA100730). One of the authors (S.T.S.) was supported by an NCRR T32 Training Grant (RR007073). Another (C.K.M.) was supported by an F32 from the National Cancer Institute (CA130458-01).

References

1. Grill V, Martin TJ. Hypercalcemia of malignancy. Rev Endocr Metab Disord 2000;1:253–263. [PubMed: 11706739]
2. Taylor GP, Matsuoka M. Natural history of adult T-cell leukemia/lymphoma and approaches to therapy. Oncogene 2005;24:6047–6057. [PubMed: 16155611]
3. Fournier PG, Chirgwin JM, Guise TA. New insights into the role of T cells in the vicious cycle of bone metastases. Curr Opin Rheumatol 2006;18(4):396–404. [PubMed: 16763461]
4. Kingsley LA, Fournier PG, Chirgwin JM, Guise TA. Molecular biology of bone metastasis. Mol Cancer Ther 2007;6:2609–2617. [PubMed: 17938257]
5. Shibata H, Abe M, Hiura K, et al. Malignant B-lymphoid cells with bone lesions express receptor activator of nuclear factor-kappaB ligand and vascular endothelial growth factor to enhance osteoclastogenesis. Clin Cancer Res 2005;11:6109–6115. [PubMed: 16144909]
6. Mitra-Kaushik S, Harding JC, Hess JL, Ratner L. Effects of the proteasome inhibitor PS-341 on tumor growth in HTLV-1 Tax transgenic mice and Tax tumor transplants. Blood 2004;104:802–809. [PubMed: 15090453]
7. Feuer G, Zack JA, Harrington WJ Jr, et al. Establishment of human T-cell leukemia virus type I T-cell lymphomas in severe combined immunodeficient mice. Blood 1993;82:722–731. [PubMed: 8338942]
8. Richard V, Nadella MV, Green PL, et al. Transcriptional regulation of parathyroid hormone-related protein promoter P3 by ETS-1 in adult T-cell leukemia/lymphoma. Leukemia 2005;19:1175–1183. [PubMed: 15889157]
9. Luchin A, Suchting S, Merson T, et al. Genetic and physical interactions between microphthalmia transcription factor and PU.1 are necessary for osteoclast gene expression and differentiation. J Biol Chem 2001;276:36703–36710. [PubMed: 11481336]
10. Han JH, Choi SJ, Kurihara N, Koide M, Oba Y, Roodman GD. Macrophage inflammatory protein-1alpha is an osteoclastogenic factor in myeloma that is independent of receptor activator of nuclear factor kappaB ligand. Blood 2001;97:3349–3353. [PubMed: 11369623]

11. Richard V, Luchin A, Brena RM, Plass C, Rosol TJ. Quantitative evaluation of alternative promoter usage and 3′ splice variants for parathyroid hormone-related protein by real-time reverse transcription-PCR. Clin Chem 2003;49:1398–1402. [PubMed: 12881458]
12. Holven KB, Damas JK, Yndestad A, et al. Chemokines in children with heterozygous familiar hypercholesterolemia: selective upregulation of RANTES. Arterioscler Thromb Vasc Biol 2006;26:200–205. [PubMed: 16254204]
13. Okada Y, Tsukada J, Nakano K, Tonai S, Mine S, Tanaka Y. Macrophage inflammatory protein-1alpha induces hypercalcemia in adult T-cell leukemia. J Bone Miner Res 2004;19:1105–1111. [PubMed: 15176993]
14. Dewan MZ, Terashima K, Taruishi M, et al. Rapid tumor formation of human T-cell leukemia virus type 1-infected cell lines in novel NOD-SCID/gammac (null) mice: suppression by an inhibitor against NF-kappaB. J Virol 2003;77:5286–5294. [PubMed: 12692230]
15. Reinholt FP, Hultenby K, Oldberg A, Heinegard D. Osteopontin–a possible anchor of osteoclasts to bone. Proc Natl Acad Sci USA 1990;87:4473–4475. [PubMed: 1693772]
16. Nosaka K, Miyamoto T, Sakai T, Mitsuya H, Suda T, Matsuoka M. Mechanism of hypercalcemia in adult T-cell leukemia: overexpression of receptor activator of nuclear factor kappaB ligand on adult T-cell leukemia cells. Blood 2002;99:634–640. [PubMed: 11781248]
17. Guise TA, Kozlow WM, Heras-Herzig A, Padalecki SS, Yin JJ, Chirgwin JM. Molecular mechanisms of breast cancer metastases to bone. Clin Breast Cancer 2005;5 Suppl. 2:S46–S53. [PubMed: 15807924]
18. Shen X, Falzon M. PTH-related protein modulates PC-3 prostate cancer cell adhesion and integrin subunit profile. Mol Cell Endocrinol 2003;199:165–177. [PubMed: 12581888]
19. Nakashima M, Ohtsuru A, Luo WT, et al. Expression of parathyroid hormone-related peptide in human thyroid tumours. J Pathol 1995;175:227–236. [PubMed: 7738719]
20. Ikeda K, Inoue D, Okazaki R, Kikuchi T, Ogata E, Matsumoto T. Parathyroid hormone-related peptide in hypercalcemia associated with adult T cell leukemia/lymphoma: molecular and cellular mechanism of parathyroid hormone-related peptide overexpression in HTLV-I-infected T cells. Miner Electrolyte Metab 1995;21:166–170. [PubMed: 7565442]
21. Liao J, McCauley LK. Skeletal metastasis: established and emerging roles of parathyroid hormone-related protein (PTHrP). Cancer Metastasis Rev 2006;25:559–571. [PubMed: 17165129]
22. Richard V, Rosol TJ, Foley J. PTHrP gene expression in cancer: do all paths lead to Ets? Crit Rev Eukaryot Gene Expr 2005;15:115–132. [PubMed: 16022632]
23. Nadella MV, Dirksen WP, Nadella KS, et al. Transcriptional regulation of parathyroid hormone-related protein promoter P2 by NF-kappaB in adult T-cell leukemia/lymphoma. Leukemia 2007;21:1752–1762. [PubMed: 17554373]
24. Arnulf B, Villemain A, Nicot C, et al. Human T-cell lymphotropic virus oncoprotein Tax represses TGF-beta 1 signaling in human T cells via c-Jun activation: a potential mechanism of HTLV-I leukemogenesis. Blood 2002;100:4129–4138. [PubMed: 12393612]
25. Terpos E, Anagnostopoulos A, Kastritis E, Bamias A, Tsionos K, Dimopoulos MA. Abnormal bone remodelling and increased levels of macrophage inflammatory protein-1 alpha (MIP-1alpha) in Waldenström macroglobulinaemia. Br J Haematol 2006;133:301–304. [PubMed: 16643432]
26. Mori K, Chano T, Yamamoto K, Matsusue Y, Okabe H. Expression of macrophage inflammatory protein-1alpha in Schwann cell tumors. Neuropathology 2004;24:131–135. [PubMed: 15139590]
27. Choi SJ, Cruz JC, Craig F, et al. Macrophage inflammatory protein 1-alpha is a potential osteoclast stimulatory factor in multiple myeloma. Blood 2000;96:671–675. [PubMed: 10887133]
28. Choi SJ, Oba Y, Gazitt Y, et al. Antisense inhibition of macrophage inflammatory protein 1-alpha blocks bone destruction in a model of myeloma bone disease. J Clin Invest 2001;108:1833–1841. [PubMed: 11748267]
29. Oyajobi BO, Franchin G, Williams PJ, et al. Dual effects of macrophage inflammatory protein-1alpha on osteolysis and tumor burden in the murine 5TGM1 model of myeloma bone disease. Blood 2003;102:311–319. [PubMed: 12649140]
30. Henderson JE, Amizuka N, Warshawsky H, et al. Nucleolar localization of parathyroid hormone-related peptide enhances survival of chondrocytes under conditions that promote apoptotic cell death. Mol Cell Biol 1995;15:4064–4075. [PubMed: 7623802]

31. Zheng F, Liang H, Liu R, et al. Parathyroid hormone-related protein regulates osteoclast inhibitory lectin expression via multiple signaling pathways in osteoblast-like cells. Endocrine 2009;35:47–56. [PubMed: 18987998]
32. Hofbauer LC, Gori F, Riggs BL, et al. Stimulation of osteoprotegerin ligand and inhibition of osteoprotegerin production by glucocorticoids in human osteoblastic lineage cells: potential paracrine mechanisms of glucocorticoid-induced osteoporosis. Endocrinology 1999;140:4382–4389. [PubMed: 10499489]
33. Halladay DL, Miles RR, Thirunavukkarasu K, Chandrasekhar S, Martin TJ, Onyia JE. Identification of signal transduction pathways and promoter sequences that mediate parathyroid hormone 1–38 inhibition of osteoprotegerin gene expression. J Cell Biochem 2001;84:1–11. [PubMed: 11746511]
34. Thirunavukkarasu K, Miles RR, Halladay DL, et al. Stimulation of osteoprotegerin (OPG) gene expression by transforming growth factor-beta (TGF-beta). Mapping of the OPG promoter region that mediates TGF-beta effects. J Biol Chem 2001;276:36241–36250. [PubMed: 11451955]
35. Gao Y, Wu X, Terauchi M, et al. T cells potentiate PTH-induced cortical bone loss through CD40L signaling. Cell Metab 2008;8:132–145. [PubMed: 18680714]
36. Ortega N, Behonick D, Stickens D, Werb Z. How proteases regulate bone morphogenesis. Ann NY Acad Sci 2003;995:109–116. [PubMed: 12814943]
37. Klein G, Vellenga E, Fraaije MW, Kamps WA, de Bont ES. The possible role of matrix metalloproteinase (MMP)-2 and MMP-9 in cancer, e.g. acute leukemia. Crit Rev Oncol Hematol 2004;50:87–100. [PubMed: 15157658]
38. Elkington PT, O'Kane CM, Friedland JS. The paradox of matrix metalloproteinases in infectious disease. Clin Exp Immunol 2005;142:12–20. [PubMed: 16178851]
39. Giraudon P, Vernant JC, Confavreux C, Belin MF, Desgranges C. Matrix metalloproteinase 9 (gelatinase B) in cerebrospinal fluid of HTLV-1 infected patients with tropical spastic paraparesis. Neurology 1998;50:1920. [PubMed: 9633766]
40. Giraudon P, Szymocha R, Buart S, et al. T lymphocytes activated by persistent viral infection differentially modify the expression of metalloproteinases and their endogenous inhibitors, TIMPs, in human astrocytes: relevance to HTLV-I-induced neurological disease. J Immunol 2000;164:2718–2727. [PubMed: 10679113]
41. Mori N, Sato H, Hayashibara T, et al. Human T-cell leukemia virus type I Tax transactivates the matrix metallo-proteinase-9 gene: potential role in mediating adult T-cell leukemia invasiveness. Blood 2002;99:1341–1349. [PubMed: 11830485]
42. Cho NH, Hong KP, Hong SH, Kang S, Chung KY, Cho SH. MMP expression profiling in recurred stage IB lung cancer. Oncogene 2004;23:845–851. [PubMed: 14647437]
43. Miyata Y, Iwata T, Maruta S, et al. Expression of matrix metalloproteinase-10 in renal cell carcinoma and its prognostic role. Eur Urol 2007;52:791–797. [PubMed: 17207914]
44. Mathew R, Khanna R, Kumar R, et al. Stromelysin-2 overexpression in human esophageal squamous cell carcinoma: potential clinical implications. Cancer Detect Prev 2002;26:222–228. [PubMed: 12269770]
45. Haeusler G, Walter I, Helmreich M, Egerbacher M. Localization of matrix metalloproteinases (MMPs), their tissue inhibitors, and vascular endothelial growth factor (VEGF) in growth plates of children and adolescents indicates a role for MMPs in human postnatal growth and skeletal maturation. Calcif Tissue Int 2005;76:326–335. [PubMed: 15868281]

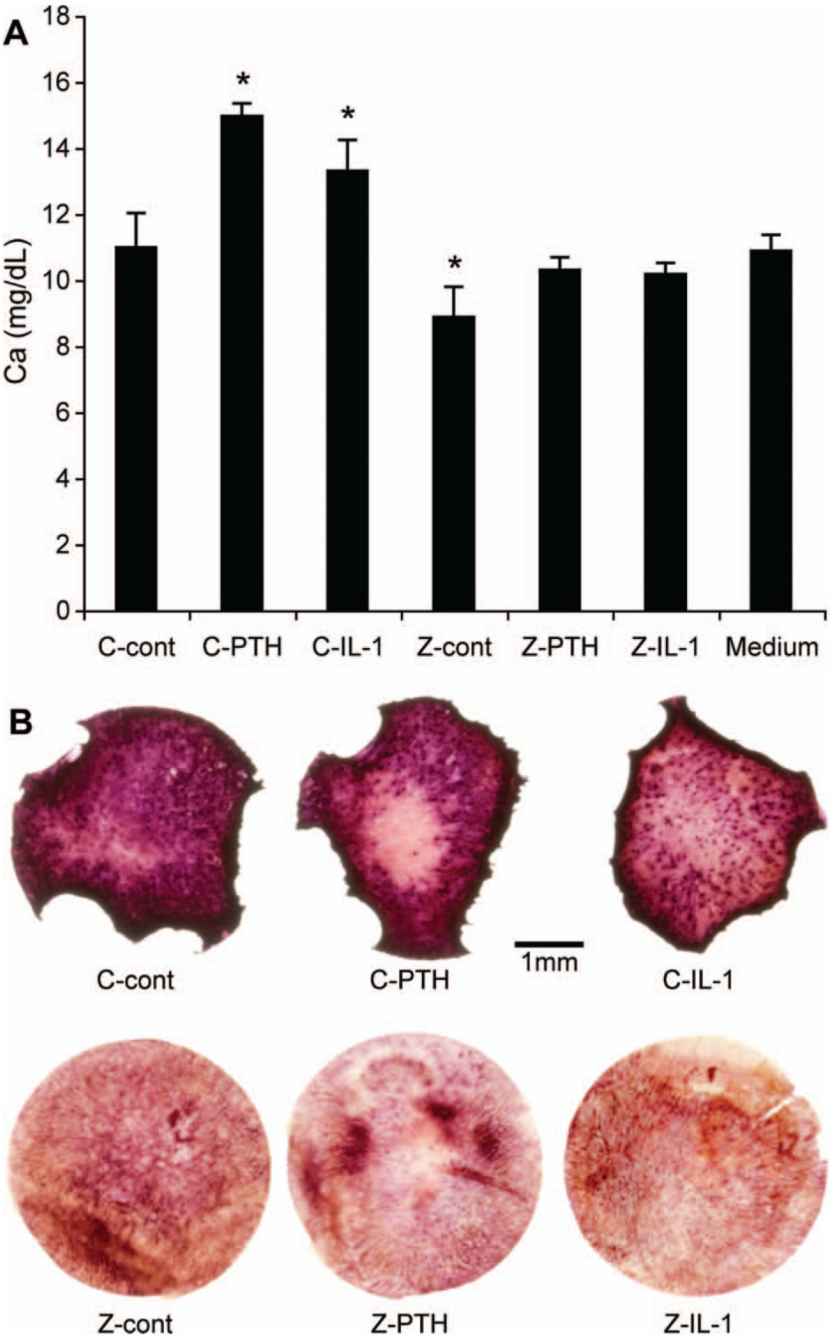

Figure 1.

Calcium concentration as an indicator of osteoclastic activity *ex vivo*. (A) Calcium concentrations in culture media of calvaria treated with PTH (10 nM) or IL-1 (2 ng/mL) for 6 days with (Z) or without (C) overnight pretreatment with zoledronic acid (Z). The symbol '*' indicates significant differences when compared to C-cont (control). Calcium concentration in medium without calvaria is also shown. (B) TRAP staining on whole-mounted calvaria. Activated osteoclasts were stained dark red.

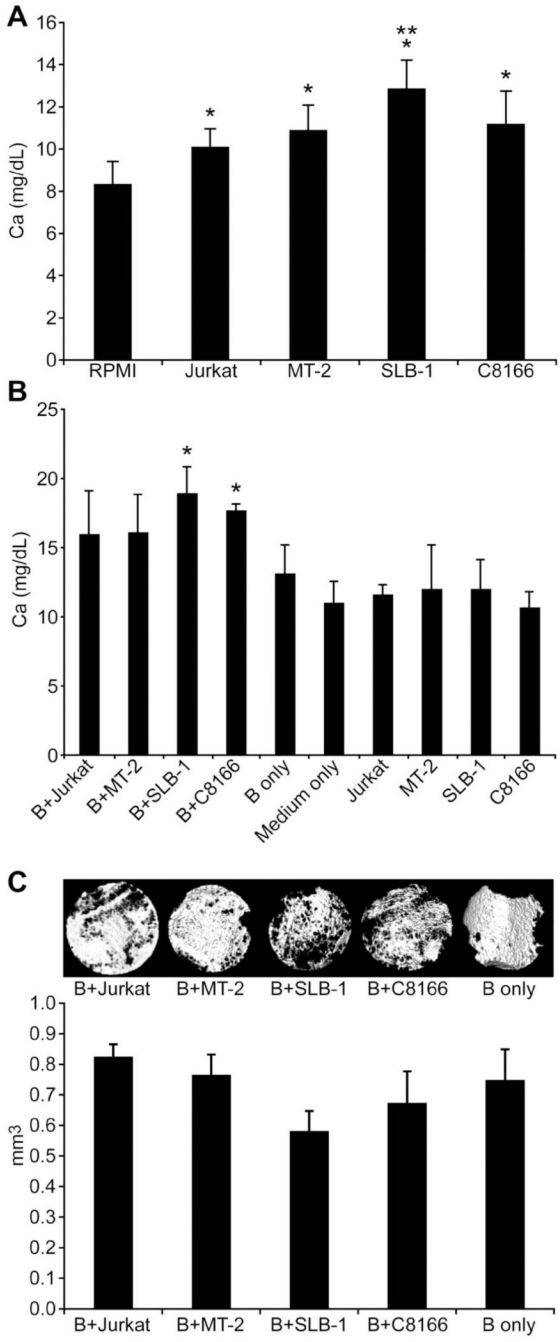

Figure 2.

HTLV-1-infected cells induced osteoclast activity *ex vivo*. (A) Calcium concentrations in culture media of calvaria treated with 25% conditioned media from 2-day cultures of HTLV-1-infected or Jurkat cells as indicated. The symbol '*' indicates significant differences when compared to RPMI (medium alone). The symbol '**' indicates significant differences when compared to Jurkat cells. (B) Calcium concentrations in culture media of calvaria co-cultured with 20 000 HTLV-1-infected cells, calvaria alone, or cells alone for 6 days. The symbol '*' indicates significant differences when compared to bone (indicated by B) alone. (C) Upper panel: μCT images of calvaria co-cultured with HTLV-1-infected cells, Jurkat cells, or bone alone; lower panel: quantitative data from μCT analysis.

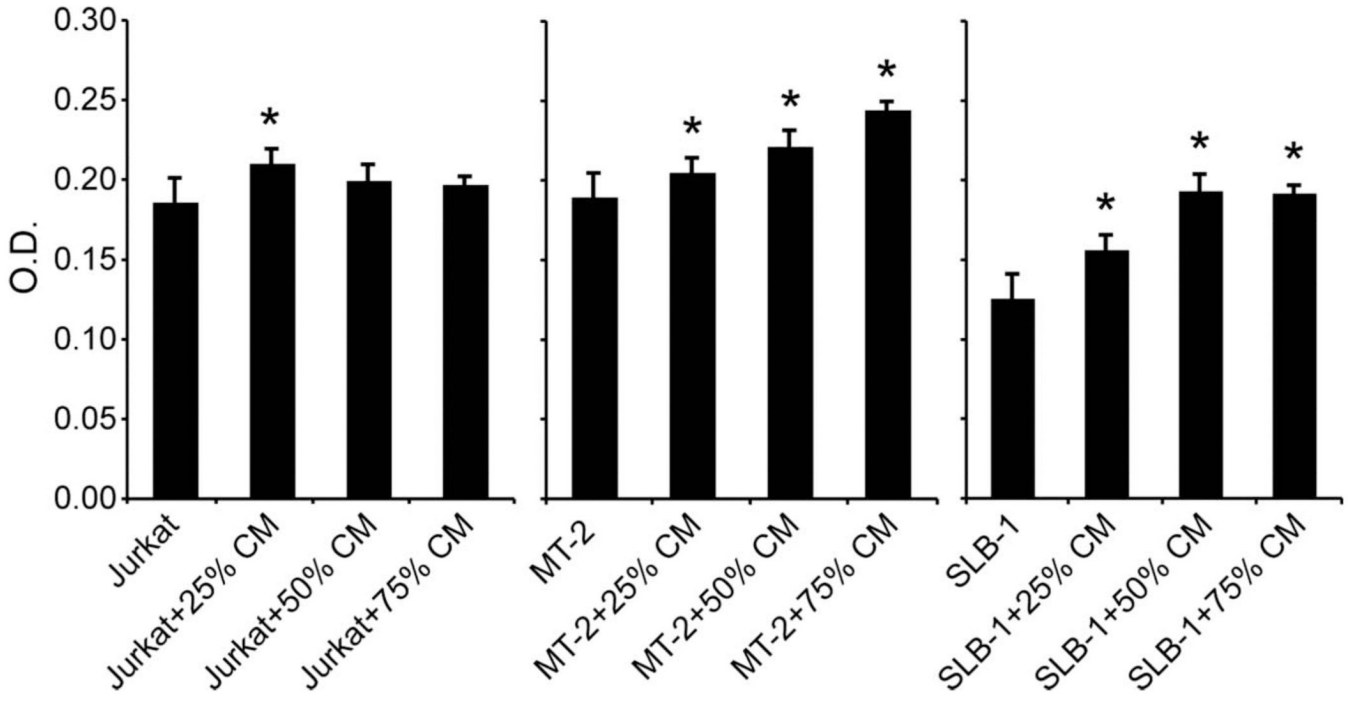

Figure 3.

Factors released from bone increased proliferation of HTLV-1-infected cells. Cell proliferation assays were performed with HTLV-1-infected (MT-2 and SLB-1) and Jurkat cells treated with 25, 50, or 75% bone-conditioned media obtained from 6-day calvaria cultures. The symbol '*' indicates significant differences when compared to cells alone.

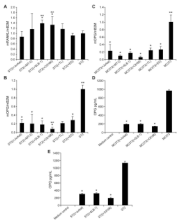

Figure 4.

T-cells affected RANKL and OPG levels in co-cultured pre-osteoblasts. Real-time RT-PCR results of (A) RANKL and (B) OPG in co-cultured pre-osteoblast ST2 cells. The symbol '*' indicates $p < 0.05$ when compared to ST2 cells. The symbol '**' indicates $p < 0.05$ when compared to ST2 (þ Jurkat). (C) Real-time RT-PCR results of OPG in co-cultured pre-osteoblast MC3T3 cells. The symbol '*' indicates $p < 0.05$ when compared to MC3T3 cells. Secreted OPG concentrations in conditioned media from (D) T-cells and ST2 cells and (E) T-cells and MC3T3 cell co-cultures. The symbol '*' indicates $p < 0.05$ when compared to ST2 or MC3T3 cells alone.

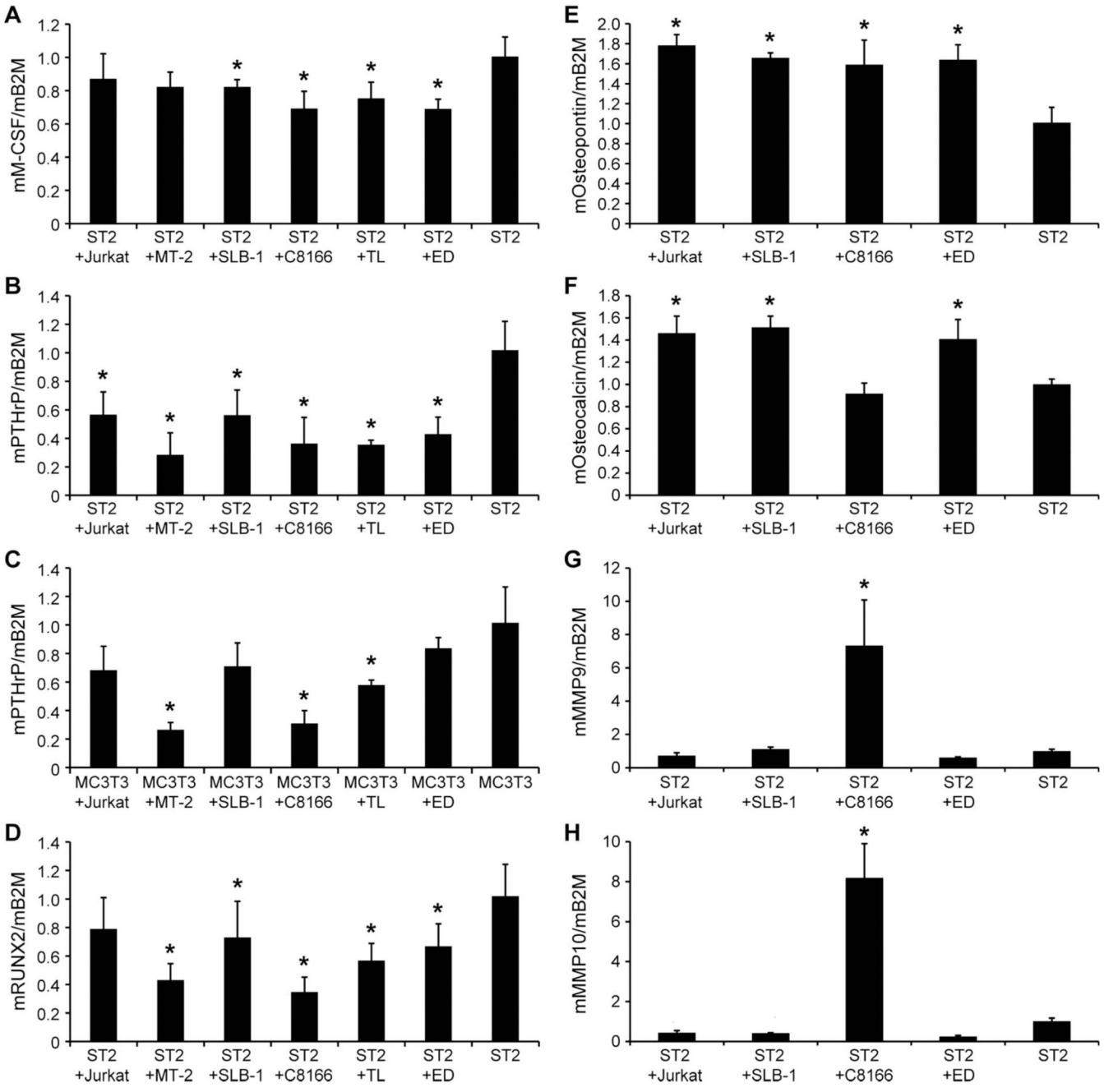

Figure 5.

T-cells affected the levels of osteoclast regulators in co-cultured pre-osteoblasts. Real-time RT-PCR of mouse M-CSF, PTHrP, RUNX2, osteopontin, osteocalcin, MMP-9, and MMP-10 in co-cultured pre-osteoblast ST2 or MC3T3 cells. The symbol '*' indicates $p < 0.05$ when compared to ST2 or MC3T3 cells alone.

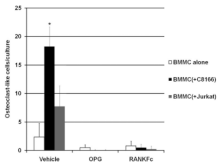

Figure 6.

Inhibitory effects of OPG and RANKFc on osteoclastogenesis induced by HTLV-1-infected T-cells. *Ex vivo* osteoclastogenesis assays were performed using mouse BMMCs co-cultured with or without T-cells. Vehicle, OPG, or RANKFc was added into the cultures for 12 days. Transwell plates were stained for TRAP. Osteoclast-like cells were identified by light microscopy and counted in three random fields in each transwell under × 100 magnification. The symbol '*' indicates $p < 0.05$ when compared to BMMCs alone treated with vehicle.

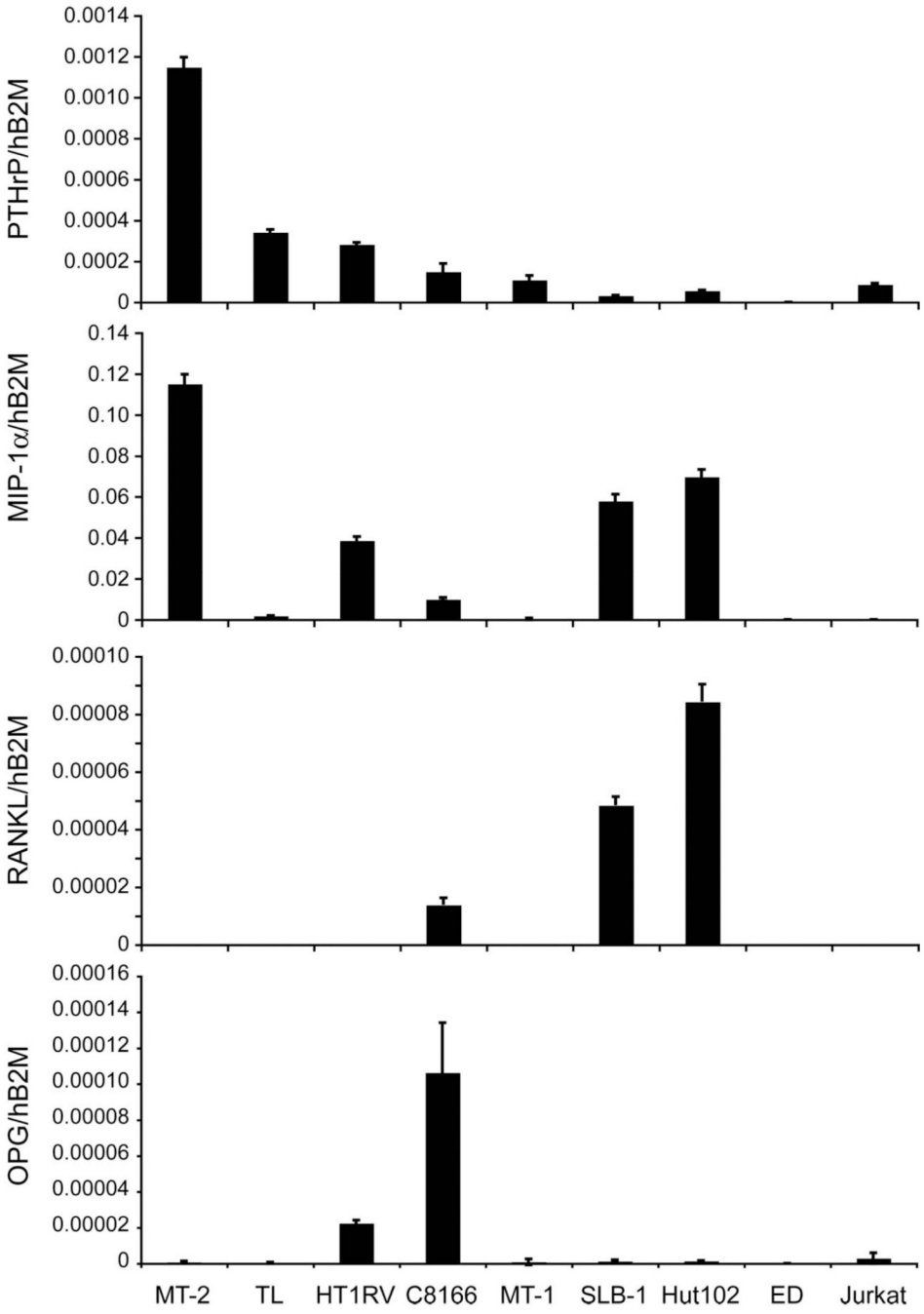

Figure 7.

HTLV-1-infected T-cells expressed PTHrP and MIP-1α mRNA. Comparison of PTHrP, MIP-1α, RANKL, and OPG mRNA expression by real-time RT-PCR in HTLV-1-infected cells and Jurkat cells. See Table I for concentrations of PTHrP and MIP-1α secreted into conditioned media.

Table I

Characteristics of HTLV-1-infected cell lines.

			In vivo characteristics			
Cells	**Origin**	**Tax expression**	**Growth**	**HHM**	**PTHrP (pM)**	**MIP-1α (pg/mL)**
MT-2	IT	+	s.c., i.m.	–	5.6	19 500
TL	L	−	s.c., i.m., i.p.	–	3.0	280
HT1RV	L + IT	+	Not yet tested	Not yet tested	6.3	5600
C8166	IT	+	Not yet tested	Not yet tested	2.9	21 600
MT-1	L	−	Not yet tested	Not yet tested	4.4	3.5
SLB-1	IT	+	s.c., i.m.	–	2.8	20 600
Hut102	IT	+	s.c., i.m.	–	4.8	25 100
ED	L	−	s.c., i.m.	–	3.8	3

HTLV-1, human T lymphotropic virus type 1; L, leukemic; IT, *in vitro* transformed; −, negative; +, positive; s.c., subcutaneous; i.m., intramuscular; i.p., intraperitoneal; HHM, humoral hypercalcemia of malignancy; PTHrP, parathyroid hormone-related protein; MIP-1α, macrophage inflammatory protein-1α. Modified from [14].

Leuk Lymphoma. Author manuscript; available in PMC 2011 March 15.